Biochimica et Biophysica Acta 1838 (2014) 2357–2368

Contents lists available at ScienceDirect

Biochimica et Biophysica Acta

journal homepage: www.elsevier.com/locate/bbamem

The effects of the C-terminal amidation of mastoparans on their biological actions and interactions with membrane-mimetic systems

Alessandra V.R. da Silva [a], Bibiana M. De Souza [a], Marcia P. dos Santos Cabrera [d], Nathalia B. Dias [a], Paulo C. Gomes [a], João Ruggiero Neto [b], Rodrigo G. Stabeli [c], Mario S. Palma [a,*]

[a] Institute of Biosciences of Rio Claro, Universidade Estadual Paulista (UNESP), C.E.I.S./Department of Biology, Rio Claro, SP, Brazil
[b] IBILCE - Universidade Estadual Paulista (UNESP), Campus of São José do Rio Preto, Department of Physics, São José do Rio Preto, SP, Brazil
[c] CEBio, Núcleo de Saúde (NUSAU), Universidade Federal de Rondônia (UNIR), Porto Velho, RO, Brazil
[d] IBILCE - Universidade Estadual Paulista (UNESP), Department of Chemistry and Environmental Sciences, São José do Rio Preto, SP, Brazil

ARTICLE INFO

Article history:
Received 17 March 2014
Received in revised form 10 June 2014
Accepted 13 June 2014
Available online 21 June 2014

Keywords:
Mastoparan
Antimicrobial peptide
H/D exchange
Mass spectrometry
Peptide–membrane interaction
Peptidomics

ABSTRACT

Polycationic peptides may present their C-termini in either amidated or acidic form; however, the effects of these conformations on the mechanisms of interaction with the membranes in general were not properly investigated up to now. Protonectarina-MP mastoparan with an either amidated or acidic C-terminus was utilized to study their interactions with anionic and zwitterionic vesicles, using measurements of dye leakage and a combination of H/D exchange and mass spectrometry to monitor peptide–membrane interactions. Mast cell degranulation, hemolysis and antibiosis assays were also performed using these peptides, and the results were correlated with the structural properties of the peptides. The C-terminal amidation promotes the stabilization of the secondary structure of the peptide, with a relatively high content of helical conformations, permitting a deeper interaction with the phospholipid constituents of animal and bacterial cell membranes. The results suggested that at low concentrations Protonectarina-MP interacts with the membranes in a way that both terminal regions remain positioned outside the external surface of the membrane, while the α-carbon backbone becomes partially embedded in the membrane core and changing constantly the conformation, and causing membrane destabilization. The amidation of the C-terminal residue appears to be responsible for the stabilization of the peptide conformation in a secondary structure that is richer in α-helix content than its acidic congener. The helical, amphipathic conformation, in turn, allows a deeper peptide–membrane interaction, favoring both biological activities that depend on peptide structure recognition by the GPCRs (such as exocytosis) and those activities dependent on membrane perturbation (such as hemolysis and antibiosis).

1. Introduction

Antimicrobial peptides (AMPs) have inspired the development of novel antimicrobial agents against resistant microorganisms. Many investigations have focused on the design of novel peptides that present increased antimicrobial activity, compared to the natural ones used as models, without damaging the cells of the host organisms, which are generally mammals [1]. The improvements in the level of antimicrobial activity have been developed in parallel with efforts to eliminate side-effects, such as the cytotoxicity against mammalian cells. Most of the variables considered during the engineering processes of the novel peptides generally correspond to the physicochemical parameters of these peptides, such as chain length, amphipathicity, α-helical content, net positive charge and hydrophobicity [2,3].

Mastoparans are amidated tetradecapeptides, characteristic of the venoms from social wasps, that cause mast cell degranulation and/or cell disruption; these peptides are present from two to four lysine residues in their sequences [4]. The hydrophobic nature of most of the amino acid residues in mastoparans usually leads them to adopt amphipathic α-helical conformations in micellar solvents [5] and in a membrane-bound state [6]. The cationicity of mastoparans contributes to the formation of discriminate anionic vesicles, which favor their antimicrobial activity [7–9]. The relative positioning of both cationic and hydrophobic residues within the peptides favors their interactions with the zwitterionic membranes of mammalian cells, and, therefore, some of these peptides can cause mast cell degranulation and hemolysis [8].

Different mechanisms to explain the actions of antibacterial peptides are currently understood: (i) in the barrel-stave model, monomers of the peptides associate with each other to form a bundle of helices that are embedded in the membrane, forming a transmembrane channel [10,11]; and, (ii) in the carpet model, the peptides act like detergents, forming eventually toroidal pores [12,13]. In both models,

* Corresponding author at: Institute of Biosciences, Universidade Estadual Paulista (UNESP), C.E.I.S./Department of Biology, Rio Claro, SP, Brazil. Tel.: +55 19 35264163; fax: +55 19 35264365.
E-mail address: mspalma@rc.unesp.br (M.S. Palma).

http://dx.doi.org/10.1016/j.bbamem.2014.06.012
0005-2736/

the physicochemical properties of the peptides, such as the length, charge distribution, net charge, molecular volume, amphipathicity and oligomeric state in solution, play essential roles in the interactions between the peptide and the membrane surface and/or with the membrane core.

The number and distribution of amino acid residues along the sequence influence the amphipathicity and net positive charge of the peptides, which in turn affect the interaction between the mastoparans and the membranes. It was previously reported that the deamidation of the C-terminus of the membrane-active peptide EMP-AF1 reduces its antimicrobial potency [5], while suppressing its hemolytic activity [14].

The enhanced potency of inflammatory peptides with amidated C-terminal residues is attributed to the increased positive charge at the N-terminus, which appears to promote the interaction between these peptides and the predominantly negatively-charged bacterial membranes [15–18]. This aspect facilitates the interaction between the peptides and the cell membrane, leading to membrane permeabilization [19].

Solution-phase hydrogen/deuterium (H/D) exchange, in combination with electrospray ionization mass spectrometry (ESI-MS), has become a useful tool for studying protein structure, protein–protein interactions, and the assignment of protein–membrane interfacial regions [20]. To investigate the role of the C-terminus of mastoparan peptides, either as an amide or as a free acid, in determining the molecular structures and biological activities of these peptides, the mastoparan peptide Protonectarina-MP [21] was used as molecular model. The secondary structures of both forms of this peptide were investigated using CD spectroscopy and molecular modeling. Peptides with an either amidated or acidic C-terminus were utilized to study their interactions with anionic and zwitterionic vesicles, using measurements of dye leakage and a combination of H/D exchange and mass spectrometry to monitor peptide–membrane interactions. Mast cell degranulation, hemolysis and antibiosis assays were also performed using these peptides, and the results were correlated with the structural properties of the peptides.

2. Material and methods

2.1. Peptide synthesis and HPLC purification

The peptides, Protonectarina-MP-NH_2 (INWKALLDAAKKVL-NH_2) and its analogue Protonectarina-MP-OH (INWKALLDAAKKVL-OH), were prepared by step-wise manual solid phase synthesis, using N-9-fluorophenylmethoxy-carbonyl (Fmoc) chemistry and Novasyn TGS resin (Novabiochem). The side-chain protective groups included β-t-butyl ester for aspartic acid, N-β-trityl for asparagine and t-butoxycarbonyl for lysine. Cleavage of the peptide–resin complexes was performed by treatment with trifluoroacetic acid (TFA)/1, 2-ethanedithiol/anisole/phenol/water (82.5:2.5:5:5:5 by volume), using 10 mL per gram of the complex at room temperature for 2 h. After filtering to remove the resin, anhydrous diethyl ether (Sigma) at 4 °C was added to the soluble material to precipitate the crude peptide, which was collected as a pellet by centrifugation at 1000 ×*g* for 15 min at room temperature. The crude peptides were dissolved in water and chromatographed under RP-HPLC, using a semi-preparative column (Shiseido C18, 250 × 10 mm, 5 μm) under isocratic elution with different concentrations of the mobile phase: 53% (v/v) acetonitrile in water [containing 0.1% (v/v) TFA] for Protonectarina-MP-NH_2; and 38% (v/v) acetonitrile in water [containing 0.1% (v/v) TFA] for Protonectarina-MP-OH. The elution was monitored at 214 nm with a UV-DAD detector (Shimadzu, mod. SPD-M10A). The homogeneity and correct sequences of the synthetic peptides were assessed using a gas-phase sequencer, PPSQ-21A (Shimadzu), based on automated Edman degradation chemistry and ESI-MS analysis.

2.2. Mast cell degranulation

Degranulation was determined by measuring the release of the granule marker, β-D-glucosaminidase, which co-localizes with histamine, as previously described [22]. Mast cells were obtained by the peritoneal washing of female adult Wistar rats. Mast cells were washed three times by re-suspension and centrifugation in a mast cell medium [150 mM NaCl (Merck), 4 mM KCl (Merck), 4 mM NaH_2PO_4 (Synth), 3 mM KH_2PO_4 (Synth), 5 mM glucose (Synth), 15 μM BSA (Sigma), 2 mM $CaCl_2$ (Merck), and 50 μL Liquemine (5000 UI/0.250 mL) (Roche)]. The cells were incubated with various peptide concentrations for 15 min at 37 °C, and, following centrifugation, the supernatants were assayed for β-D-glucosaminidase activity. Briefly, 50 μL of substrate (5 mM p-nitrophenyl-N-acetyl-β-D-glucosaminidine in 0.2 M citrate, pH 4.5) and 50 μL of medium samples were incubated in 96-well plates for 6 h at 37 °C to yield the chromophore p-nitrophenol. After incubation, 50 μL of the previous solution was added to 150 μL of 0.2 M Tris, and the absorbance was measured at 405 nm. The values were expressed as the percentage of total β-D-glucosaminidase activity from rat mast cell suspensions, determined in lysed mast cells in the presence of 0.1% (v/v) Triton X-100 (considered to be the 100% reference point). The results were compared to the activities measured for the standard mast cell degranulating peptide HR2 (Sigma). The cell suspensions in the absence of any peptide were used as negative controls. The results are expressed as the means ± SD of five experiments.

2.3. Mast cell lysis

Mast cell lysis was assayed by measuring the leakage of lactate dehydrogenase (LDH) from the mast cell cytoplasm; the LDH assay was performed as previously described [23]. The cells utilized in this assay were the same as those used in mast cell degranulation assay, described above. LDH activity was assayed by using the UV-LDH Assay Kit (Biobras Diagnostics); 20 μL of each supernatant was pre-incubated with 800 μL of LDH buffer (50 mM Tris pH 7.4, containing 1.2 mM pyruvate and 5 mM EDTA) for 5 min, at 37 °C. The reaction was initiated by the addition of 200 μL of LDH substrate (0.15 mM NADH); the kinetics of NADH consumption were monitored by recording the decrease in absorbance at 340 nm over 3 min (Δ A340) at 37 °C. The results were initially calculated as catalytic units (μmol NADH min^{-1} at 37 °C and pH 7.4) and then converted into relative activity, compared to the total LDH activity of rat mast cells lysed in the presence of 0.1% (v/v) Triton X-100 (considered to be the 100% reference point). The results are expressed as the means ± SD of five experiments.

2.4. Hemolysis

Five hundred microliters of washed rat red blood cells (WRRBC) was suspended in 50 mL of physiological saline solution [0.9% (w/v) NaCl]. Ninety microliters of this suspension was incubated with 10 μL of peptide solution at different concentrations, at 37 °C for 2 h. The samples were then centrifuged, and the supernatants were collected; the absorbance values of the supernatants were measured at 540 nm. The absorbance measured from lysed WRRBC in the presence of 1% (v/v) Triton X-100 was considered to be 100%. The results are expressed as the means ± SD of five experiments.

2.5. Antimicrobial activity

The minimal inhibitory concentration (MIC) of the peptides was determined based on the methods previously described by Meletiadis and colleagues [24]. The following microorganisms were used: *Staphylococcus aureus* (CCT 2580), *Bacillus cereus* (ATCC 11778), *Escherichia coli* (CCT 1457), and *Pseudomonas aeruginosa* (ATCC 15422). The experiment was performed in 96-well plates. Bacterial cells were suspended in sterile culture medium; the inoculum size was 1×10^4 cells/mL in

Müller–Hinton broth (DIFCO), confirmed by the use of the McFarland scale. From this culture, 50 μL was spread onto a microplate previously containing 50 μL of Müller–Hinton broth, resulting in a final cell density of 1.5×10^3 cells/mL. Cells were incubated at 37 °C for 18 h in the presence of 100 μL of each peptide solution, at concentrations ranging from 0.24 to 500 μg/mL. After incubation, 10 μL of a triphenyltetrazolium chloride (TTC) (Mallinckrodt) solution (final concentration 0.05% w/v) was added to each plate. The plates were incubated at 37 °C for 24 h, and, after incubation, 20 μL of a triphenyltetrazolium chloride solution (TTC) 0.5% (w/v) was added. The plates were then incubated for an additional period of 2 h at 37 °C. The minimal inhibitory concentration was defined as the concentration at which the dye level was not reduced; oxytetracycline, at concentrations ranging from 0.24 to 500 μg/mL, was used as a control. The results are expressed as the means ± SD of five experiments.

2.6. Liposome preparation

Homogeneous films were made with pure egg L-α-phosphatidylcholine (PC) or a 70:30 molar ratio mixture of PC and egg L-α-phosphatidyl-DL-glycerol (PG), both supplied by Sigma-Aldrich. The films were obtained by dissolving the phospholipids in a small volume of chloroform (1–2 mL), evaporated under N_2 flux in round bottom flasks, and completely dried under vacuum for at least 3 h. These films were hydrated with ultrapure water at a final phospholipid concentration of 5 mM for H/D exchange mass spectrometry analysis; or with 5 mM Tris/H_3BO_3 buffer, containing 0.5 mM EDTA and 150 mM NaF, pH 7.5, for CD spectroscopy analysis; or with 10 mM Tris/HCl buffer, containing either 25 mM carboxyfluorescein (CF) for leakage experiments or 150 mM NaCl for fluorescence spectroscopy. The suspension was sonicated with a titanium-tipped sonifier (40 W), under N_2 flux, in an ice/water bath for 50 min (or until clear) to produce small unilamellar vesicles (SUVs). Titanium debris was removed by centrifugation. Large unilamellar vesicles (LUVs), used in dye release experiments and tryptophan fluorescence spectroscopy, were obtained by two extrusion steps using an Avanti Mini-Extruder (Alabaster, AL, USA) and double-stacked polycarbonate membranes (Nuclepore Track-etch Membrane, Whatman); the suspension was passed 6 times through 0.4 μm membranes and then 11 times through 0.1 μm membranes. For the dye-entrapped LUVs, free dye was separated by gel filtration on a Sephadex G25 M column (Amersham Biosciences). LUVs were used within 48 h of preparation. SUVs were used immediately following preparation. The lipid concentration was determined by phosphorus analysis [25]. Laser light scattering measurements, with a Zeta Sizer Nano NS-90 (Malvern Instruments), revealed homodisperse LUVs in suspension, with an average diameter of 105.0 ± 0.2 nm, among several preparations.

2.7. Circular Dichroism (CD) measurements

CD spectra were obtained using a 20 μM peptide concentration in different environments: in water; in Tris/H_3BO_3 buffer, containing 0.5 mM EDTA and 150 mM NaF, pH 7.5; in 40% (v/v) 2,2,2-trifluoroethanol (TFE)/bi-distilled water; in sodium dodecyl sulfate solutions (SDS), above and below the critical micellar concentration (CMC) (8 mM and 165 μM, respectively); in 100 μM PC; and in 100 μM PCPG SUVs. CD spectra were recorded from 260 to 190 nm or 200 nm with a Jasco-815 spectropolarimeter (JASCO International Co. Ltd., Tokyo, Japan), which was routinely calibrated at 290.5 nm using d-10-camphorsulfonic acid solution. Spectra were acquired at 25 °C using 0.5 cm path length cell and averaged over nine scans, at a scan speed of 20 nm/min, bandwidth of 1.0 nm, 0.5 s response and 0.1 nm resolution. Following baseline correction, the observed ellipticity, θ (mdeg) was converted to mean residue ellipticity [Θ] (degcm^2/dmol) using the relationship: $[\Theta] = 100\ h/(lcn)$; where l is the path length in centimeters, c is the peptide millimolar concentration, and n is the number of peptide bonds. Assuming a two-state model, the observed mean residue ellipticity at 222 nm ($[\Theta]_{222}$ obs) was converted into an α-helix fraction (f_α), using the method proposed by Rohl and Baldwin [26].

2.8. Molecular modeling

The modeling procedure began with an alignment of the target peptide sequence with Mastoparan-X (PDB ID: 2CZP), a related peptide of known three-dimensional (3D) structure, as a template [27]. Homologous structures for the peptides Protonectarina-MP-NH_2 and Protonectarina-MP-OH, among known structural templates in the PDB (Protein Data Bank), were identified using BLASTP [28,29]. This alignment was formatted to be the input for the program MODELER. The output is a 3D model for each target sequence containing all main-chain and side-chain non-hydrogen atoms. Several slightly different models can be calculated by varying the initial structure. To build the models, MODELLER 8 v.2 was used [30]. For each peptide, a total of 1000 models were created, and the stereochemical quality of the models was assessed by the program PROCHECK [31]. The final models were selected with 100% residues in favored regions of the Ramachandran plot, with the best values for the overall G factor and the lower values of energy minimization. The images were constructed using the graphics programs MolMol [32] and VMD 1.8.6 [33].

2.9. Dye leakage

An aliquot of the LUV suspension was injected into a 1 cm quartz cell, containing magnetically stirred peptide solutions in Tris/HCl buffer (10 mM, EDTA 1 mM and 150 mM NaCl), at peptide concentrations ranging from 0.5 to 45 μM, for a final volume of 1.2 mL; suspensions were added according to the permeabilizing efficiency, to achieve approximately 100% leakage within 20–30 min of contact time. The release of carboxyfluorescein (CF) from the vesicles was fluorometrically monitored using an ISS PC1 spectrofluorometer (Urbana Champaign, IL, USA), in which the emission was set at 520 nm and the slit width was set at 0.5 nm (excited at 490 nm, 1 nm slit width). To determine the decrease in self-quenching at 25 °C, the percentage of dye leakage was calculated after regular time intervals, with the equation: percentage of leakage $= 100 \times (F - F_0) / (F_{100} - F_0)$; where F is the observed fluorescence intensity; and F_0 and F_{100} correspond, respectively, to the fluorescence intensities in the absence of peptides and to 100% leakage, as determined by the addition of 20 μL of a 10% Triton X-100 solution. The results are expressed as the means ± SD of three experiments.

2.10. ESI mass spectrometry

Mass spectrometric analyses were performed in a triple quadrupole mass spectrometer (Micromass, Mod. Quattro II). The experimental protocol was based on previously described methods [34] and adapted to the present investigation. The mass spectrometer was outfitted with a standard probe electrospray (ESI, Micromass, Altrincham, UK). The samples were injected into the electrospray transport solvent with a microsyringe (250 μL) coupled to a microinfusion pump (KD Scientific) at a flow rate of 4 μL/min. The mass spectrometer was calibrated with intact horse heart myoglobin and its typical cone-voltage induced fragments to operate at a resolution of 4000. The samples were analyzed by positive electrospray ionization (ESI) using typical conditions: a capillary voltage of 3.5 kV; a cone-voltage of 52 V; a desolvation gas temperature of 80 °C; and flow of nebulizer gas (nitrogen) of approximately 20 L/h and drying gas (nitrogen) at 200 L/h. The ESI mass spectra were obtained in the continuous acquisition mode, scanning from m/z 50 to 4000 at a scan time of 10 s. The data were acquired and treated using MassLynx software (Micromass). Typical conditions used to perform the CID MS experiments were: argon as the collision gas; a capillary voltage of 1.78 kV; a cone voltage of

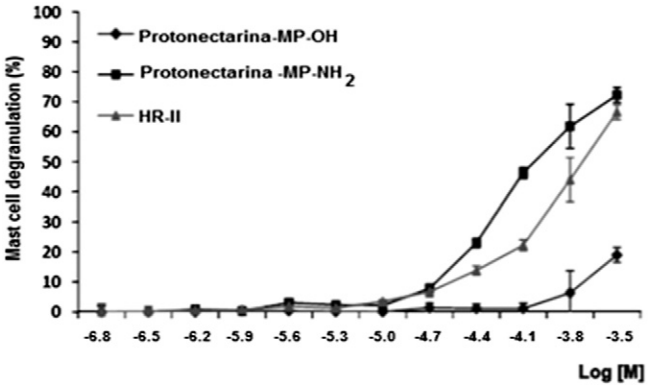

Fig. 1. Degranulation activity in rat peritoneal mast cells. The activity was determined by measuring the release of the granule marker, β-D-glucosaminidase, which co-localizes with histamine and the values for β-D-glucosaminidase released in the medium were expressed in the percentage of total β-D-glucosaminidase. Values are mean ± SD ($n = 5$).

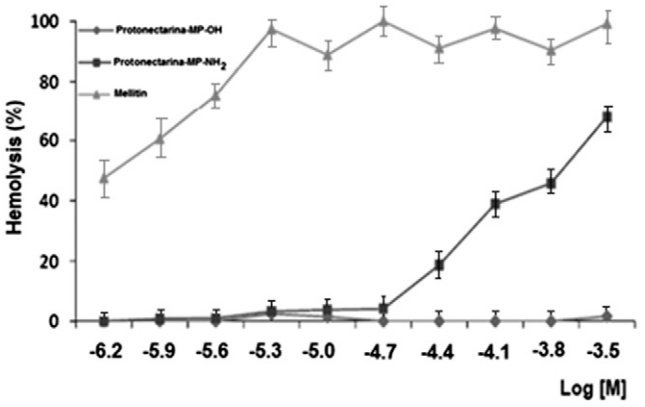

Fig. 3. Hemolytic activity in washed rat red blood cells (WRRBC). The absorbance measured at 540 nm from lysed WRRBC in the presence of 1% (v/v) Triton X-100 was considered as 100%. Values are mean ± SD ($n = 5$).

120 V; collision energy from 35 to 80 eV; collision gas pressure of 3×10^{-3} mBar; and a desolvation gas temperature of 80 °C. Peptide sequences were manually assigned from the ESI-MS/MS product ion mass spectra.

2.11. Hydrogen/deuterium exchange of free peptides and their interactive forms with liposomes

The H/D exchange assays between free peptides and peptides interacting with liposomes were performed as described previously [19]. LUVs in the presence or absence of peptides were pre-incubated for times ranging from 1 to 60 min at room temperature before measuring H/D exchange. The suspensions of liposomes in the presence of peptides were prepared for H/D exchange monitoring as described above, except for the replacement of bidistilled water with 99% (v/v) D_2O (Cambridge Isotopes Laboratories, Inc.). The free peptide solution was prepared for H/D exchange by adding 6 μL of peptide solution (1 μg/μL) to either 22 μL bidistilled water or liposome suspension and adding 50 μL 99% (v/v) D_2O following the liposome pre-incubation. The H/D exchange was allowed to proceed for 30 s and was then quenched by adjusting the pH to 2.5 by the addition of 2 μL of 88% formic acid and cooling to 0 °C. The solution of free peptides or the liposomes/peptide suspension was introduced into the mass spectrometer at a flow of 4 μL/min with a microperfusion pump (KD Scientific). Spectra were continuously acquired over 3 min by direct injection of the samples into the ionization source system. Mass spectrometric measurements were started as quickly as possible (the dead time was approximately 90 s) and analyses were performed in MS and MS/MS modes. Taking into account both the time of incubation between the free peptide/proteoliposomes and the dead time of the experiment, the first time point of each mass spectrometry measurement was acquired at 2 min and lasted until 3 min. Each H/D exchange reaction was performed three times for each condition, and the tandem mass spectra were individually acquired for each replicate experiment. The mass-to-charge values of all ions of interest from each spectrum were used to calculate the rate values, with their respective standard deviations, and for the calculation of deuterium incorporation into the peptide.

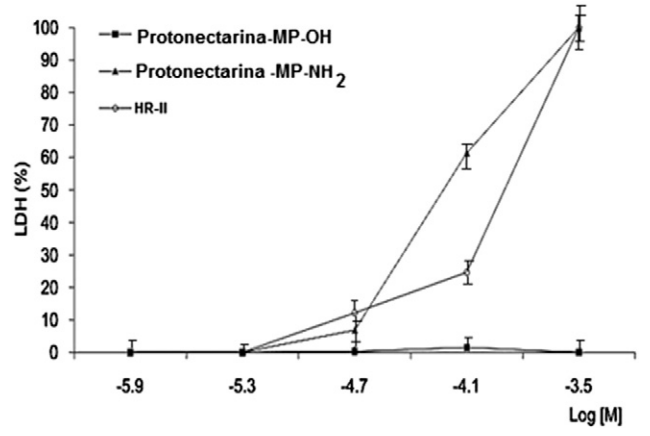

Fig. 2. Delivering of LDH activity from rat peritoneal mast cells to the incubation medium. The results were shown as relative activity by using the total LDH activity contents of rat mast cells lysed in the presence of 0.1% (v/v) Triton X-100 (considered as 100%). Results are expressed as mean ± SD ($n = 5$).

2.12. Determination of the scrambling factors for deuteron positions

The scrambling factor (SF) was calculated according to Eq. (1), as previously described [19]:

$$SF = \frac{\sum_{i}^{N} |\Delta(D_{st} - D_{co})| - \sum_{i}^{N} |\Delta(D_{st} - D_{ex})|}{\sum_{i}^{N} |\Delta(D_{st} - D_{co})|} \quad (1)$$

where: $\Delta(D_{st} - D_{co})$ — is the deviation between the deuterium content per fragment-ion, considering two virtual opposite situations: full deuteron scrambling and no scrambling; $\Delta(D_{st} - D_{ex})$ — is the deviation between the deuterium content per fragment-ion in the virtual full deuteron scrambling and the experimental values obtained for each set of the experimental conditions; i — represents the individual subsequent fragment-ions; and N — represents the total number of fragment

Table 1
Minimal inhibitory concentration (MIC) of the peptides Protonectarina-MP-NH_2 and Protonectarina-MP-OH compared to other wasp venom antimicrobial peptides.

Peptides	Minimal inhibitory concentration (μg/mL)			
	Gram-negative		Gram-positive	
	E. coli	*P. aeruginosa*	*S. aureus*	*B. cereus*
Protonectarina-MP-OH	62.5	>500.0	250.0	62.0
Protonectarina-MP-NH_2	7.8	62.5	15.6	7.8
Oxytetracycline	1.0	3.9	<0.2	1.0
Anoplin	50.0	20.0	5.0	20.0
Crabroline	150.0	>500.0	>500.0	75.0
EMP-AF	50.0	20.0	5.0	>500.0
Mastoparan-M	12.5	12.5	6.2	>500.0

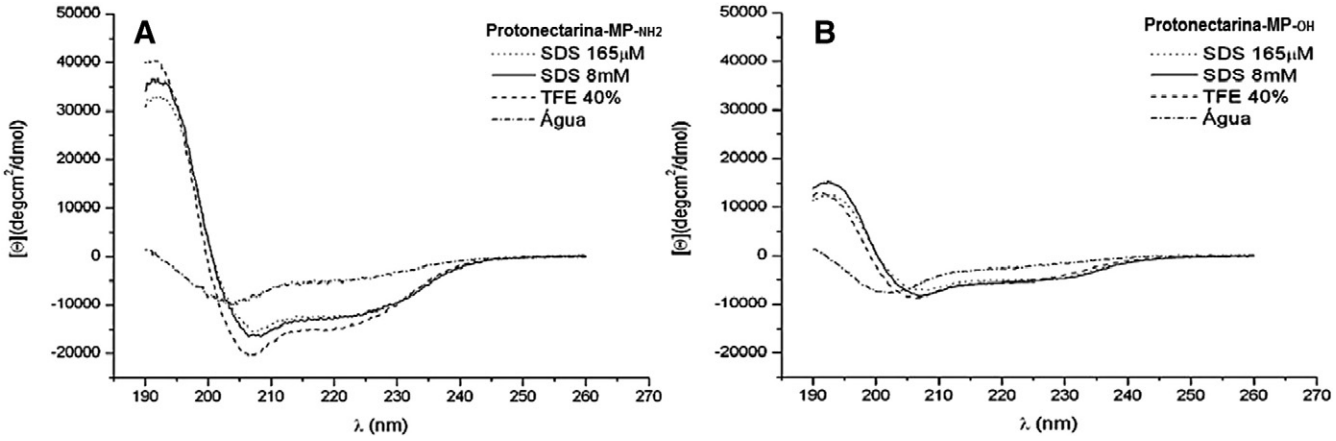

Fig. 4. CD spectra of (A) Protonectarina-MP-NH_2 and (B) Protonectarina-MP-OH obtained at 20 μM, at 25 °C, in the presence of water, 8 mM SDS and 40% (v/v) TFE. No smoothing has been applied.

peaks of which the mass increase could be determined from the CID MS spectra.

3. Results

3.1. Biological activities

Protonectarina-MP-NH_2 and Protonectarina-MP-OH were analyzed in assays for mast cell degranulation, the release of LDH activity from mast cells, hemolysis, chemotaxis of PMNLs and antimicrobial activities. Fig. 1 shows the results of rat peritoneal mast cell degranulation for both forms of Protonectarina-MP and for the standard peptide (HRII). The results revealed that Protonectarina-MP-NH_2 is a potent mast cell degranulating peptide, presenting degranulation activity ($ED_{50} = 8 \times 10^{-5}$ M) slightly higher than the standard peptide HRII ($ED_{50} = 20 \times 10^{-5}$ M). However, Protonectarina-MP-OH presented a reduced degranulation activity, even at high concentrations. Thus, it was not possible to determine the ED_{50} value for Protonectarina-MP-OH.

The lysis of rat peritoneal mast cells was monitored by measurements of LDH activity delivered to the incubation medium. This procedure was performed to determine whether the peptides could disturb the structure of the mast cell membrane; the results of this assay are shown in Fig. 2. Protonectarina-MP-NH_2 presented an elevated level of activity ($ED_{50} = 6 \times 10^{-5}$ M), which was higher than that presented by the standard peptide HR-II ($ED_{50} = 20 \times 10^{-5}$ M), while Protonectarina-MP-OH presented no activity.

Hemolysis of rat erythrocytes was also examined for both forms of Protonectarina-MP, and the results are shown in Fig. 3. Mellitin was used as the standard peptide, presenting high hemolytic activity ($ED_{50} = 6 \times 10^{-7}$ M); Protonectarina-MP-OH presented no hemolysis, while Protonectarina-MP-NH_2 presented a reduced level of hemolysis ($ED_{50} = 2 \times 10^{-4}$ M).

The antimicrobial activities of both forms of Protonectarina-MP were examined and compared to the previously reported activities of peptides derived from wasp venoms; these results are summarized in Table 1. Protonectarina-MP-NH_2 presented a potent antimicrobial activity against both Gram-positive and Gram-negative bacteria, while Protonectarina-MP-OH presented a much more reduced antimicrobial activity. The antimicrobial activity of Protonectarina-MP-NH_2 was similar to that observed for Anoplin, in relation to Gram-positive and Gram-negative bacteria, and to mastoparan-M, in relation to the Gram-positive bacteria [5].

3.2. Structure investigations

The secondary structures of Protonectarina-MP-NH_2 and Protonectarina-MP-OH were investigated by CD spectroscopy in different environments (Figs. 4 and 5). The spectra of Protonectarina-

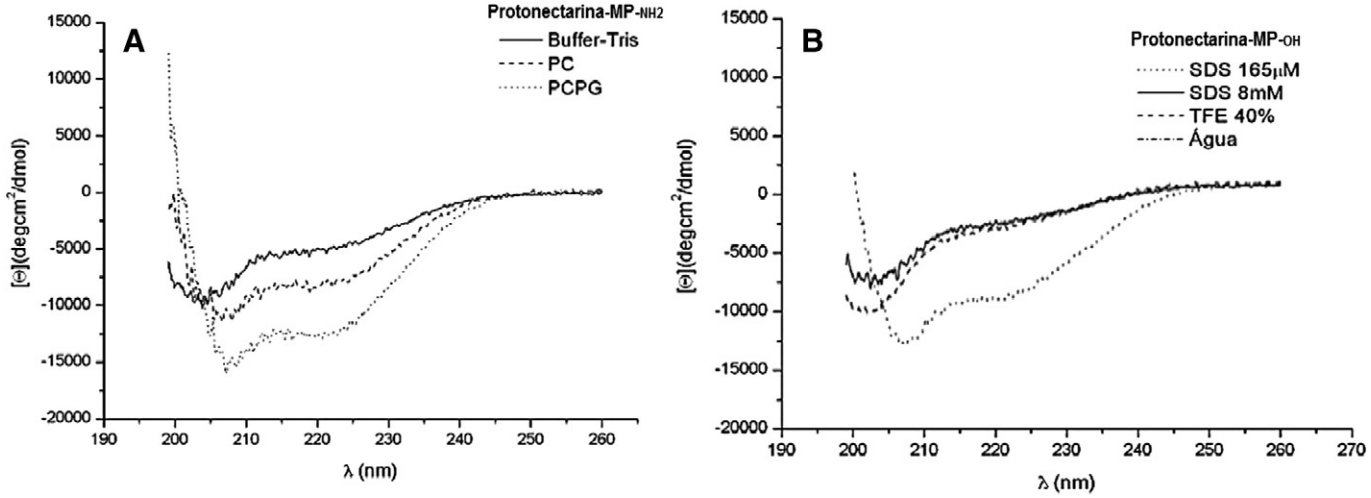

Fig. 5. CD spectra of (A) Protonectarina-MP-NH_2 and (B) Protonectarina-MP-OH obtained at 20 μM, 25 °C in the presence of buffer-Tris and SUVs made with PC and PCPG. No smoothing has been applied.

Table 2
α-Helix fraction (f_α) of the Protonectarina-MP-NH_2 and Protonectarina-MP-OH in different environments.

	Protonectarina-MP-NH_2		Protonectarina-MP-OH	
	$[\Theta_{222}]$	f_α	$[\Theta_{222}]$	f_α
Water	−4330	0.15	−2490	0.07
8 mM SDS	−12,400	0.39	−5360	0.16
40% TFE	−14,530	0.47	−5430	0.16
Tris buffer	−4970	0.15	−2190	0.06
PC	−7980	0.25	−2490	0.07
PCPG	−12,460	0.39	−6700	0.20

MP-NH_2 in water (Fig. 4A) or in Tris buffer (Fig. 5A) revealed some helical tendencies. The dichroic band at 198 nm, which is characteristic of unordered structures, was deviated to 204 nm, while a small dichroic band appeared near 222 nm. In the same environments, the spectra of Protonectarina-MP-OH were characteristic of unordered structures (Fig. 4B). The spectra of Protonectarina-MP-NH_2 and Protonectarina-MP-OH in the presence of 40% (v/v) TFE or in 8 mM SDS (Fig. 4A and B) showed negative dichroic bands at 208 and 222 nm, consistent with the induction of α-helical conformations in these media. Table 2 presents the molar ellipticity ($[\Theta_{222}]$) and the fraction of α-helices, calculated according to the two-state model for both peptides in these environments. Both peptides were clearly different in the total content of helical structures. In the presence of zwitterionic PC or anionic PCPG vesicles, the spectra of both peptides also differed in relation to the content of helical structures (Fig. 5A and B).

The induction of a higher helical content for the amidated peptide in relation to the form presenting acidic C-terminus in the presence of zwitterionic vesicles reflects a more efficient interaction between the amidated peptide and the membrane, and it is well correlated with the increased mast cell degranulation, hemolysis and LDH delivery. Additionally, the increased helical content of the amidated peptide in the presence of anionic vesicles when compared to its acidic form is well correlated with its lower MIC values (Table 1). These results indicated that C-terminal amidation is fundamental for peptide backbone structuration, i.e., for the stabilization of the secondary structure in α-helical conformations.

The secondary structures of Protonectarina-MP-NH_2 and Protonectarina-MP-OH were also analyzed by molecular modeling; 1000 models were generated and validated through the analysis of the structure by the Procheck program [31]. This analysis considered the Ramachandran plot and values of the overall G-factor. Ideally, the value of this factor should be above −0.5. Fig. 6A and C shows the molecular models of these peptides as ribbon representations, while Fig. 6B and D represents the charged surface distribution for each peptide. The G-factor values for both models were 0.26 for Protonectarina-MP-NH_2 and 0.37 for Protonectarina-MP-OH. In both models, all the residues were in the most favored regions of the Ramachandran plot, with eleven residues in the α-helical region and only a single residue at the β-sheet region (result not shown). The residues at the amino- and carboxyl-termini were not considered because they can be localized in any region of the diagram.

3.3. Investigation of the interactions with membrane-mimetic vesicles

The lytic activity of both forms of Protonectarina-MP was investigated by analyzing the leakage of carboxyfluorescein from PC and PCPG vesicles induced by each peptide. Dose–response curves revealed sigmoid profiles for Protonectarina-MP-NH_2 in the presence of either PC or PCPG vesicles, while Protonectarina-MP-OH presented the sigmoid profile only in the presence of PCPG vesicles, as shown Fig. 7A and B, respectively. The dose–response curves suggested that the peptide molecules bind and accumulate on the external surface of vesicles and cell membranes until a critical threshold concentration is reached (P/L molar ratio) (Table 3). Further peptide accumulation caused intense leakage. Fig. 7A shows the remarkable differences in the lytic activity on zwitterionic PC vesicles between amidated and carboxylated forms of Protonectarina-MP. A critical P/L concentration below 0.45 could not be determined, indicating that the amidated form was

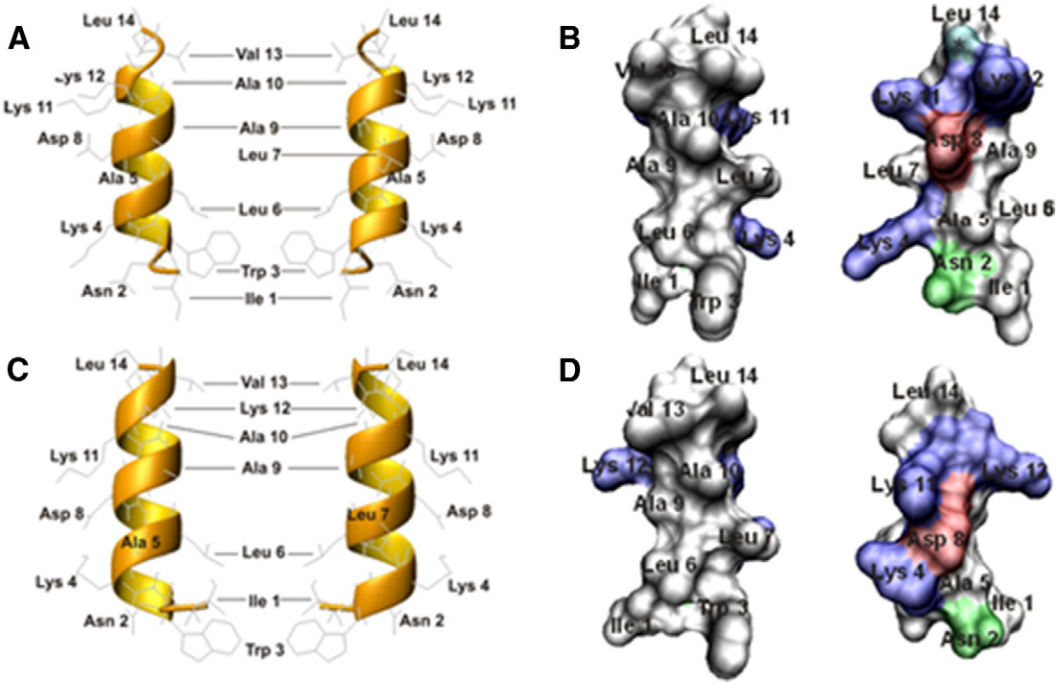

Fig. 6. Structural models of Protonectarina-MP-NH_2 (A and B) and Protonectarina-MP-OH (C and D). Two different views of closest-to-the-mean structure of residues 1–14 with side chains shown, in both ribbon representation (A and C), and as charge surface representation (B and D): negative residues are shown in red, positive in blue, hydrophilic in green and hydrophobic in white.

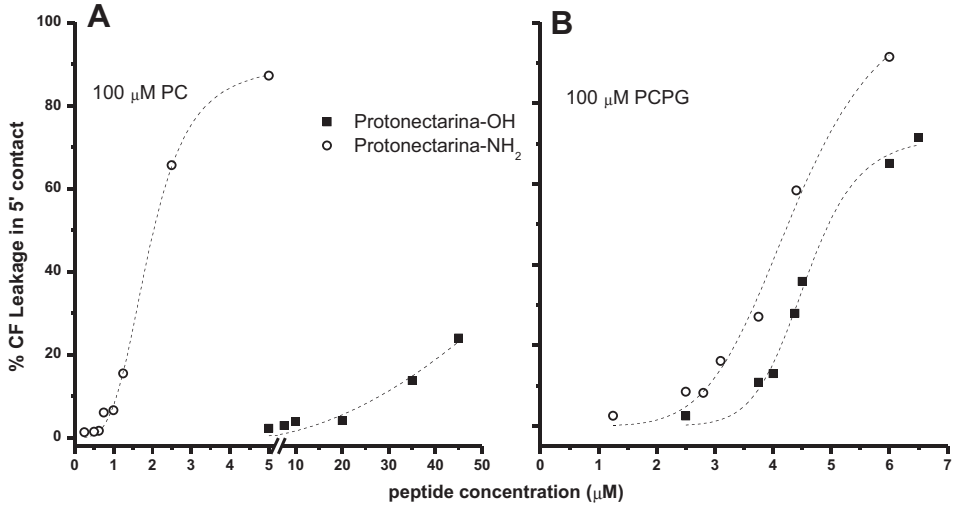

Fig. 7. Dose–response curves showing the percentage of CF leakage after 5 contact times, at 25 °C.

approximately 40 times more efficient than the carboxylated form and had stronger peptide–membrane interactions. These results are in agreement with the higher hemolytic character of the amidated form (Fig. 3) and with its higher helical content in PC vesicles (Fig. 5 and Table 2). Protonectarina-MP-NH_2 was also more lytic than Protonectarina-MP-OH in anionic PCPG vesicles. Fig. 7B shows that the carboxylated peptide was more selective towards the anionic environment.

To better understand the peptide–membrane interactions, the measurement of H/D exchange between peptides interacting with membrane-mimetic systems was used, monitored by ESI-mass spectrometry, as previously reported for other mastoparans [19]. This technique permits a site-specific determination of the deuteron positions in peptide–membrane proteoliposome systems, indicating which amino acid residues of the peptide chain are in the inner core of the membrane as well as which residues are interacting with the outside medium.

Fig. 8A shows the CID spectrum of Protonectarina-MP-NH_2 soluble in water and Fig. 8B shows the CID spectrum of the peptide soluble in 40% (v/v) D_2O. Fig. 8C to H shows the spectra of H/D exchanges in 40% (v/v) D_2O at different times of incubation, in a time course experiment in the presence of the zwitterionic membrane of PC. The spectra showed that the number of deuterons incorporated into the peptide chain varied according to time.

The residues Leu^6, Leu^7, Asp^8, Ala^9 and Ala^{10} changed their deuteration state depending on the time of incubation; meanwhile, Ile^1, Asn^2, Lys^4, Ala^5, Lys^{11}, Lys^{12}, Val^{13} and Leu-NH_2 at the C-terminus remained deuterated the entire course of incubation, in the presence of PC vesicles. The residue Trp^3 remained embedded into the membrane most of the incubation time, preventing to be deuterated. Considering the large sizes of the figures showing the tandem mass spectra of the peptides in the presence of PC and PCPG vesicles, the CID spectra of Protonectarina-MP-NH_2, in the presence of PCPG vesicles, and the CID spectra of Protonectarina-MP-OH, in the presence of PC and PCPG vesicles, are shown in the supplemental information (Figs. S1 to S3).

Fig. S1 shows the spectra of the H/D exchange of Protonectarina-MP-NH_2 in water (Fig. S1A), in the presence of PCPG vesicles and 40% (v/v) D_2O (Fig. S2B), at different incubation times from a time course incubation (Fig. S1C to H). The spectra showed that the incorporation from 8 to 11 deuterons occurred between 1 and 60 min incubation; under these conditions all residues of the peptide chain altered their H/D exchange depending on the time of incubation.

Fig. S2 shows the spectra of the H/D exchange of Protonectarina-MP-OH in water (Fig. S2A), in the presence of PC vesicles and 40% (v/v) D_2O (Fig. S2B), at different incubation times from a time course incubation (Fig. S2C to H). Under these conditions the only residues that became deuterated during all incubation time were the Ile and Leu from N- and C-termini, respectively; all the other residues altered their deuteration condition, depending on the time of incubation, in the presence of PCPG vesicles.

Fig. S3 shows the spectra of the H/D exchange of Protonectarina-MP-OH in water (Fig. S3A), in the presence of PCPG vesicles and 40% (v/v) D_2O (Fig. S3B), at different incubation times from a time course incubation (Fig. S3C to H). The spectra showed that the incorporation of 11 to 13 deuterons from 1 to 60 min incubation, where most of the amino acid residues from peptide sequence altered their H/D exchange depending on the time of incubation.

Demmers et al. [20] suggested that the extent of intramolecular hydrogen scrambling is strongly influenced by experimental factors, such as the exact amino acid sequence of the peptide, the nature of the charge carrier, and, most likely, by the gas-phase structure of the peptide ion. Some studies have reported that hydrogen mobility within peptide ions is sufficiently rapid to scramble their position, even prior to their collision during mass spectrometric analysis [35]. As H/D exchange in combination with mass spectrometry analysis under CID conditions is used more frequently for the structural and conformational investigations of proteins and peptides, it is very important to observe and to minimize the effects of deuterium scrambling in the results obtained through this technique. De Souza and Palma [19] developed a method to validate the results obtained from H/D exchange combined with CID mass spectrometry. Thus, the scrambling factor is a number defined between 0 (indicating no scrambling) and 1 (representing a state with a statistical distribution of all deuterium atoms). Table 4 shows the scrambling factors determined for the positions of deuterons in the MS/MS spectra for Protonectarina-MP-NH_2 and Protonectarina-MP-OH, in the presence of PC and PCPG vesicles (Figs. 8 and S1 to S3).

Table 3
Critical P/L molar ratios and EC_{50} (peptide concentration to reach 50% CF leakage in 5′) determined for the peptides Protonectarina-MP-NH_2 and Protonectarina-MP-OH from the leakage dose–response curves, in PC and PCPG vesicles.

	Critical P/L ratio		EC_{50} (μM)	
	PC	PCPG	PC	PCPG
Protonectarina-MP-OH	–	0.036	–	5.0
Protonectarina-MP-NH_2	0.0085	0.026	2.0	4.3

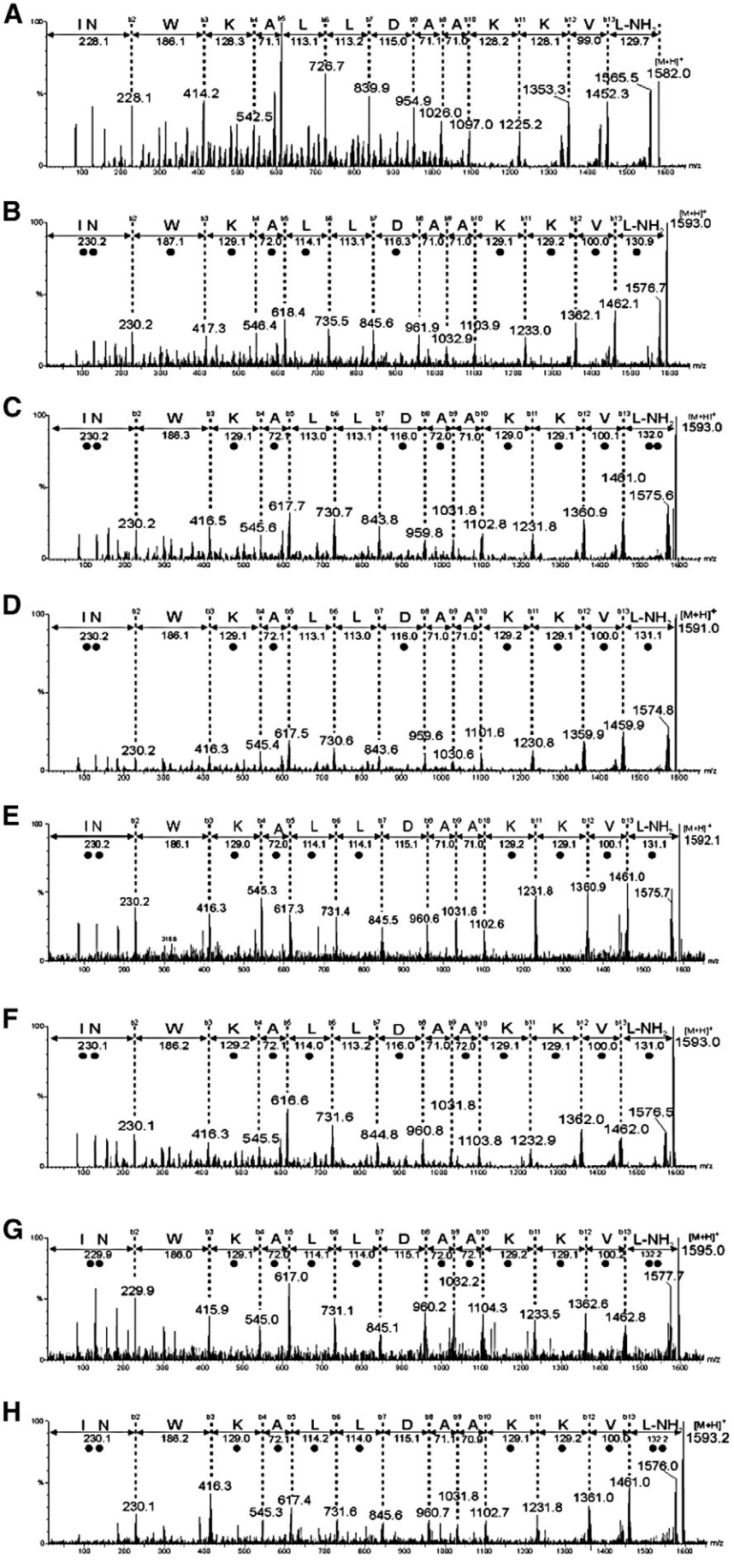
A
IN W K A L L D A A K K V L-NH2
228.1 186.1 128.3 71.1 113.1 113.2 115.0 71.1 71.0 128.2 128.1 99.0 129.7
[M+H]+ 1582.0
726.7
839.9
1565.5
1452.3
1353.3
954.9
1026.0
1097.0
1225.2
414.2
542.5
228.1
B
IN W K A L L D A A K K V L-NH2
230.2 187.1 129.1 72.0 114.1 113.1 116.3 71.0 71.0 129.1 129.2 100.0 130.9
[M+H]+ 1593.0
1576.7
1462.1
1362.1
618.4
735.5
845.6
961.9
1103.9
1233.0
1032.9
230.2
417.3
546.4
C
IN W K A L L D A A K K V L-NH2
230.2 186.3 129.1 72.1 113.0 113.1 116.0 72.0 71.0 129.0 129.1 100.1 132.0
[M+H]+ 1593.0
1461.0
1575.6
1360.9
617.7
730.7
843.8
1031.8
1102.8
1231.8
959.8
230.2
416.5
545.6
D
IN W K A L L D A A K K V L-NH2
230.2 186.1 129.1 72.1 113.1 113.0 116.0 71.0 71.0 129.2 129.1 100.0 131.1
[M+H]+ 1591.0
1574.8
1459.9
1359.9
617.5
730.6
843.6
959.6
1101.6
1230.8
1030.6
230.2
416.3
545.4
E
IN W K A L L D A A K K V L-NH2
230.2 186.1 129.0 72.0 114.1 114.1 115.1 71.0 71.0 129.2 129.1 100.1 131.1
[M+H]+ 1592.1
1461.0
1575.7
1360.9
1231.8
545.3
617.3
731.4
845.5
960.6
1031.8
1102.6
230.2
416.3
F
IN W K A L L D A A K K V L-NH2
230.1 186.2 129.2 72.1 114.0 113.2 116.0 71.0 72.0 129.1 129.1 100.0 131.0
[M+H]+ 1593.0
1576.5
1462.0
1362.0
616.6
731.6
844.8
960.8
1031.8
1103.8
1232.9
230.1
416.3
545.5
G
I N W K A L L D A A K K V L-NH2
229.9 186.0 129.1 72.0 114.1 114.0 115.1 72.0 72.1 129.2 129.1 100.1 132.2
[M+H]+ 1595.0
1577.7
1462.8
1362.6
1233.5
617.0
731.1
845.1
960.2
1032.2
1104.3
229.9
415.9
545.0
H
I N W K A L L D A A K K V L-NH2
230.1 186.2 129.0 72.1 114.2 114.0 115.1 71.1 70.9 129.1 129.2 100.0 132.2
[M+H]+ 1593.2
1576.0
1461.0
1361.0
1231.8
1031.8
617.4
731.6
845.6
960.7
1102.7
230.1
416.3
545.3

The scrambling factors changed from 0.00 to 0.38, indicating that the results and the proposed models of peptide–membrane interactions are reliable.

Based on the results obtained from H/D exchange and mass spectrometry assays reported above, it was possible to propose a peptide/membrane interaction for each experimental condition assayed. Fig. 9 shows some snapshots of the time course incubation experiment, in which some models of interaction peptide–membrane for both peptides in the presence of PC and PCPG vesicle membranes are proposed. Because the measurement of H/D exchange was performed for the amide hydrogen of each peptide bond, the positions assigned as "deuterated" in the mass spectra represent the orientation of the α-carbon backbone of each amino acid residue to the external membrane surface; the "non-deuterated" position corresponds with the embedding of the α-carbon backbone in the membrane core. Thus, the deuterated amino acid residues were positioned in the external membrane surface (assigned to the white region in the scheme shown in Fig. 9). However, the non-deuterated amino acid residues were interacting with the core of the membranes, and, therefore, were assigned to the gray region of the scheme shown in Fig. 9.

4. Discussion

Mastoparans are polycationic peptides from the venoms of social wasps, presenting amphipathic helical structures capable of inducing mast cell degranulation and/or the lysis of mast cell membranes, hemolysis and sometimes antimicrobial actions [36]. The degranulating activity appears to be related to the activation of G-protein coupled receptors in the mast cells, while the other activities mentioned above are ascribed to the ability of the peptides to interact with the cell membrane surface via the positively charged side-chains of their amphipathic α-helical structures [37].

The increased biological activities of polycationic peptides appear to be associated with the amidation of their C-terminal residues. There are studies reporting higher activities of amidated mastoparans compared with their acidic counterparts [38]; however, the precise mechanism of action for these peptides is not known yet. It is believed that the biological actions that depend on the direct interactions between the peptides and the lipid components of cell membranes (mast cell lysis, hemolysis and antibiosis) occur through either the barrel stave or the carpet-like mechanisms [39,40]. It was demonstrated that the reduced activity of the acidic form of mastoparans occurs not only due to the reduction of the net positive charge of these peptides, but also due to a structural destabilization of the amphipathic α-helix, which also affects their direct interaction with cell membranes [15].

Despite the importance of these studies, little extensive investigation has been performed focusing on the structure/activity relationship of mastoparan peptides. Structural and functional studies have always been isolated from each other; some functional investigations only assayed mast cell degranulation and/or leukocytes chemotaxis, which are mostly dependent on peptide–receptor (GPCRs) interaction [41,42]. Meanwhile, other studies have focused only on hemolytic action and/or antibiosis, which are dependent on peptide–phospholipid interaction [43,44], without investigating mast cell degranulation and PMNL chemotaxis. In addition to the raised concerns, most of these experiments were performed using different peptide sequences, making it difficult to make generalized observations.

Thus, the mastoparan peptide Protonectarina-MP was selected as a model for the investigation of the structure/activity relationship, using peptides with either an acidic (Protonectarina-MP-OH) or an amidated (Protonectarina-MP-NH_2) C-terminus. The peptides were manually synthesized in solid phase and purified using RP-HPLC under isocratic elution, and their purities were checked by ESI/MS analysis. Simulations of the secondary structures of each peptide were performed using molecular modeling by homology. Both models were considered stereochemically possible using the validation tools, Ramachandran plots and G-factors. Because these models were built based on a static helical template (Mastoparan-X; PDB ID: 2CZP), they corresponded at this level of consideration to helical molecules. Fig. 6 shows the models, where the amphiphatic character of both molecules is clear, i.e., the peptides have a predominantly hydrophobic surface, distinct from the hydrophilic ones.

Experimental data from CD spectroscopy in membrane-mimetic environments confirmed the helical structure of both Protonectarina-MP peptides in anionic PCPG vesicles, while in PC vesicles, only the amidated form assumed a helical structure. The peptide presenting a higher content of secondary structures (Protonectarina-MP-NH_2) appeared to interact more efficiently with membrane-mimetic systems than the form with a reduced level of secondary structure organization (Protonectarina-MP-OH). Experiments measuring dye leakage confirmed that Protonectarina-MP peptides may target the phospholipid matrix of either anionic or zwitterionic cell membranes, but their lytic activity appears to be influenced by the ionic character of the bilayer. Protonectarina-MP-OH presented more intense activity on anionic bilayers, while Protonectarina-MP-NH_2 was much less selective since it seems to interact both with zwitterionic and anionic membranes. The threshold P/L ratio and the leakage efficiency of these peptide–membrane interactions were found to be dependent on the vesicle surface charge density and on the net charge of the peptides.

Considering that the mode of interaction between the mastoparan peptides and the membranes is not well known, it is important to understand the effect of the amidation of the C-terminus of mastoparans on the peptide–membrane interactions. To investigate these interactions, a previously reported experimental protocol was applied in which the nascent peptide–membrane interactions could be monitored by examining peptides interacting with lipid vesicles. The peptide/vesicle mixtures were incubated in the presence of D_2O under experimental conditions that permitted the continuous monitoring of the H/D exchange of the amide protons from the solvent-exposed peptide bonds (positioned outside membrane), by ESI-MS and MS/MS analyses. In this protocol, the backbone amide sites embedded in the membrane were protected from the H/D exchange [19]. The protocol used is sensitive and powerful enough to be used as tool for investigating the architecture of short, linear, α-helical peptides at the membrane–water interface of vesicles, while they are interacting with the membranes [19]. In this type of protocol, some extension of intramolecular deuterium scrambling may occur, which could potentially affect the precision of information regarding the correct positioning of the amide protons in the peptide backbone exposed to the solvent. To evaluate the reliability of each reported deuterium location at the peptide bonds, and to validate the models of the global positioning of the α-carbon backbone of the peptides in relation to the external medium and membrane core of the vesicles when interacting with PC and PCPG vesicles, the scrambling factors for all of the CID spectra obtained for each incubation condition were determined. This factor is a number between 0 (no

Fig. 8. CID MS spectra of Protonectarina-MP-NH_2, acquired under continuous infusion of the peptide solution or liposome suspension in the presence of peptide (in PC vesicles) into the mass spectrometer. Each spectrum represents the combination of scans within 1 min of data acquisition at different incubation conditions: (A) peptide soluble in water in the absence of D_2O (molecular ion at m/z 1582.0 as $[M + H]^+$); (B–H) peptide soluble in the presence of 40% D_2O (v/v) (molecular ion at m/z 1593.0 as $[M + H]^+$) at different times, after quenching the H/D exchange; peptide as proteoliposome in PC vesicles, in the presence of 40% D_2O (v/v) incubated during (B) 1 min, (C) 3 min, (D) 5 min, (E) 10 min, (F) 15 min, (G) 30 min and (H) 60 min, and after quenching the H/D exchange (molecular ion at m/z 1593.0 as $[M + H]^+$, 1591.0 as $[M + H]^+$, 1592.0 as $[M + H]^+$, 1546.0 as $[M + H]^+$, 1595.0 as $[M + H]^+$ and 1593.0 as $[M + H]^+$, respectively). The mass differences between the consecutive b_n fragment-ions and their correspondence to the deduced amino acid sequences are shown. The black spots assigned under the symbols of some amino acid residues correspond to the location of deuterons at specific amide hydrogens.

Table 4
Scrambling factors determined for the positions of deuterons in the tandem mass spectra acquired for the peptides Protonectarina-MP-NH_2 and Protonectarina-MP-OH under interaction with PC and PCPG vesicles.

Time (min)	Protonectarina-MP-NH_2		Protonectarina-MP-OH	
	PC	PCPG	PC	PCPG
1	0.25	0.25	0.00	0.05
3	0.35	0.38	0.23	0.08
5	0.38	0.37	0.27	0.28
10	0.32	0.10	0.20	0.30
15	0.28	0.08	0.14	0.23
30	0.31	0.32	0.07	0.17
60	0.10	0.27	0.35	0.29

scrambling) and 1 (representing a complete scrambling) [19]. Table 4 shows that the scrambling factors changed from 0.00 to 0.38, indicating that the results from the present investigation and the proposed models of peptide–membrane interactions are reliable (Fig. 9).

The results summarized in Fig. 9 show that under the conditions assayed, both peptides interacted in parallel to the membrane surface and were not fully internalized into the lipid layer. The α-carbon backbone of both peptides formed a twisted structure, in which some regions became exposed to the solvent outside of the membrane, while other regions of this backbone were internalized in the membrane. The total number of amino acid residues contained in the regions embedded in the membrane provides us with information regarding how strong the peptide–membrane interaction is. Thus, it is clear that both peptides interacted better with the anionic vesicles (PCPG) than with the zwitterionic vesicles (PC), most likely due to the stabilization of the supra-molecular structure between the peptide and the membrane when the negative charges of the anionic membranes neutralize the positive charges of the peptides. Protonectarina-MP-NH_2 interacted better with both types of the membranes than Protonectarina-MP-OH. Thus, the peptide with an amidated C-terminus embedded from 3 to 5 residues into the PC membrane (with a rate value of 3.6), while the peptide with an acidic C-terminus embedded from 0 to 3 residues (with a rate value of 1.4) during the 60 min incubation. Protonectarina-MP-NH_2 interacted with the anionic membranes (PCPG), embedding from 3 to 5 residues into the membrane (with rate value of 4.7), while Protonectarina-MP-OH embedded from 1 to 3 residues (with a rate value of 2.7).

Some interesting features observed in these experiments were as follows: i) the N-terminus of both peptides always remained positioned outside of the membrane during most of the incubation time for both forms of the peptide; ii) the C-terminus (including the neighbor region) remained exposed to the outside membrane most of the time, for both forms of the peptide, except near the 10 min incubation time for Protonectarina-MP-NH_2 with PCPG vesicles; and iii) amino acid residues presenting hydrophobic side-chains, such as the residue of Trp, became embedded into the membrane from 3 min of incubation until the end of the experiment for Protonectarina-MP-NH_2; this occurred only a few times in the incubations of Protonectarina-MP-OH with both types of vesicles.

The H/D exchange experiments were performed with [P]/[L] of 1/100, i.e., in a non-lytic condition. Consequently, the experiment enabled the visualization of peptide movements on the vesicle membranes at different times, without membrane rupture. The positioning of each peptide at different times of incubation is schematized in Fig. 9 (and also in Figs. S1 to S3).

The interpretation of the sketch shown in Fig. 9 suggests that each model proposed at different times of incubation just represents a snapshot of a long time course experiment (60 min), which initiated with the Protonectarina-MP peptides incubated in water and in the presence of the vesicles; under this condition the peptides presented a randomly coiled chain (as demonstrated in Table 2). After a short time, the peptide adsorbs to the lipid membrane in an orientation more-or-less parallel to its surface. The positioning of the amide bonds protected from H/D exchange suggests that one or more peptide populations were adsorbed to the vesicles. These populations, characterized by different contacts with the bilayer are not "frozen" and along the incubation time the conformations of these populations change to optimize the amphipathicity, leading to conformations more energetically favorable. A careful observation of the models for the peptide–membrane interaction proposed in Fig. 9 reveals the unusual insertion of charged side-chains of Asp and Lys residues into the hydrophobic core of the membrane, which causes membrane destabilization and contributes to the occurrence of frequent conformational changes in the central region of peptide chain. Thus, considering that both N- and C-termini remain positioned outside of the membrane during most of the incubation time course, the frequent conformational changes in the middle of peptide chain would contribute to the bilayer destabilization.

The positioning of the peptides in the bilayer under these condition is not "frozen", therefore the peptide molecules may eventually diffuse on the membrane surface during all the experiment; under these conditions, some regions of the membranes reach a critical concentration of peptides, followed by the consequent leakage of vesicles. These results support the hypothesis that the interaction of Protonectarina-MP-NH_2 and Protonectarina-MP-OH with PC and PCPG membranes occurs through the carpet model.

Orioni et al. [45] used a combination of fluorescence spectroscopy and molecular dynamic simulations to determine that the antimicrobial peptide PMAP-23C (which belongs to the group of cathelicidins) interacts with the PCPG membrane vesicles by inserting itself below the polar head groups of the phospholipids, with its chain orientated parallel to the plane of the bilayer. They proposed that the mechanism of bilayer destabilization involves an unusual insertion of charged side-chains into the hydrophobic core of the membrane, like those reported above in the present investigation. Milik and Skolnick [46] combined techniques of Monte Carlo dynamic simulation with a hydropathy scale method for the prediction of the association and the orientation of the peptides in relation to the membrane surface. Thus, a model of interaction was proposed between Magainin-2 with biological membranes in general, in which the peptide adsorbs on the membrane surface forming a helical structure, which inserts some parts of the α-carbon backbone into the core of the membrane, changing constantly the conformation, but always maintaining its positioning almost parallel in relation to the external surface of the membrane. This model of peptide–membrane interaction seems to be very similar to that proposed above for the Protonectarina-MP peptides.

The biological assays revealed that Protonectarina-MP-NH_2 caused potent mast cell degranulation followed by the delivery of a small amount of LDH activity from the cytoplasm of mast cells, indicating that the delivery of the content from the granules is mainly due to mast cell degranulation, with a small contribution from mast cell membrane perturbation. The amidated peptide also caused a small amount of hemolysis in rat erythrocytes, in a similar manner to that reported above for the mast cells. The acidic form of Protonectarina-MP presented none of the biological activities reported for the amidated peptide. Protonectarina-MP-NH_2 was a very active antibiotic peptide for both Gram-positive and Gram-negative bacteria, while Protonectarina-MP-OH was poorly active under the same conditions. The amidation of the C-terminal residue appears to be responsible for the stabilization of the peptide conformation in a secondary structure that is richer in α-helix content than its acidic congener. The helical, amphipathic conformation, in turn, allows a deeper peptide–membrane interaction to occur, favoring both biological activities that depend on ligand (peptide) structure recognition by the GPCRs (such as exocytosis) and those activities dependent on membrane perturbation (such as hemolysis and antibiosis).

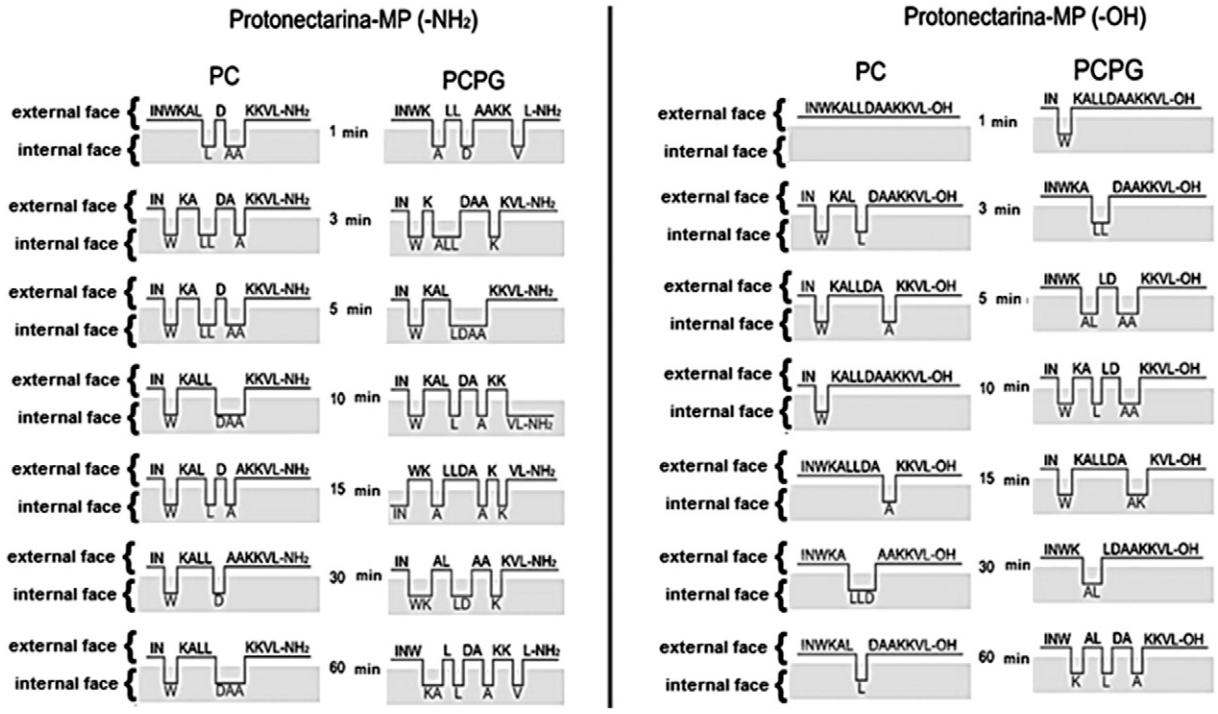

Fig. 9. Scheme representing the interpretation models for the snapshots of the mass spectrometric analysis, showing the positioning of the α-carbon backbone of the peptides Protonectarina-MP-NH_2 and Protonectarina-MP-OH under interaction with PC and PCPG vesicles, in relation to the external medium and membrane core of the vesicles.

5. Conclusions

The acidic or amidated condition of the C-terminal residue of the mastoparans seems to influence the stabilization of these polycationic peptides, and consequently their interactions with the target membranes and/or the receptors located at these membranes. To investigate the role of the C-terminus either as an amide or as a free acid, in determining the molecular structures and biological activities of these peptides, the mastoparan peptide Protonectarina-MP was used as molecular model. The secondary structures of both forms of this peptide were investigated using CD spectroscopy and molecular modeling. Peptides presenting amidated or acidic C-terminus were studied in relation to their interactions with anionic (PCPG) and zwitterionic vesicles (PC), using measurements of dye leakage and a combination of H/D exchange and mass spectrometry to monitor peptide–membrane interactions. The C-terminal amidation promotes the stabilization of the secondary structure of the peptide with a relatively high content of helical conformations, when compared to the peptide presenting acidic C-terminus, permitting a deeper interaction of the amidated mastoparan with the phospholipid constituents of animal and bacterial cell membranes. Mast cell degranulation, hemolysis and antibiosis assays were also performed using these peptides, and the results were correlated with the structural properties of the peptides, i.e., the amidated form of Protonectarina-MP was much more active than the acidic ones. The results also suggested that Protonectarina-MP interacts with the membranes in a way that both terminal regions remain positioned outside the external surface of the membrane, while the α-carbon backbone becomes partially embedded in the membrane core and changing constantly the conformation, and causing membrane destabilization.

Conflict of interest statement

All authors have no financial or personal relationships with other people or organizations that could inappropriately influence our work.

Acknowledgements

This research is supported by grants from FAPESP (BIOprospecTA proc. 04/07942-2, 11/51684-1), CNPq, Instituto Nacional de Ciência e Tecnologia de Investigação em Imunologia- iii (INCT/CNPq-MCT), and CAPES (Rede Nanobiotec-Brasil). MSP, RGS and JRN are researchers for the Brazilian Council for Scientific and Technological Development (CNPq).

Appendix A. Supplementary data

Figures S1 to S3 show the CID spectra of Protonectarina-MP-NH_2 in the presence of PCPG vesicles and the CID spectra of Protonectarina-MP-OH in the presence of PC and PCPG vesicles. This material is available free of charge via the Internet at www.elsevier.com.

Appendix A. Supplementary data

Supplementary data to this article can be found online at http://dx.doi.org/10.1016/j.bbamem.2014.06.012.

References

[1] M.M. Javadpour, M.M. Juban, W.C. Lo, S.M. Bishop, J.B. Alberty, S.M. Cowell, C.L. Becker, M.L. McLaughlin, De novo antimicrobial peptides with low mammalian cell toxicity, J. Med. Chem. 39 (1996) 3107–3113.
[2] M. Dathe, T. Wideprecht, Structural features of helical antimicrobial peptides: their potential to modulate activity on model membranes and biological cells, Biochim. Biophys. Acta 1462 (1999) 71–87.
[3] M. Dathe, J. Meyer, M. Beyermann, B. Maul, C. Hoischen, M. Bienert, General aspects of peptide selectivity towards lipid bilayers and cell membranes studied by variation of the structural parameters of amphipathic helical model peptides, Biochim. Biophys. Acta 1558 (2002) 171–186.
[4] T. Nakajima, Pharmacological biochemistry of vespid venoms, in: T. Piek (Ed.), Venoms of the Hymenoptera: Biochemical, Pharmacological and Behavioural Aspects, Academic Press Inc. Ltd., London, 1986, pp. 309–327.
[5] M.P. dos Santos Cabrera, B.M. de Souza, R. Fontana, K. Konno, M.S. Palma, W.F. de Azevedo Jr., J. Ruggiero Neto, Conformation and lytic activity of Eumenine Mastoparan: a new antimicrobial peptide from wasp venom, J. Pept. Res. 64 (2004) 95–103.

[6] Y. Hori, M. Demura, M. Iwadate, A.S. Ulrich, T. Niidome, H. Aoyagi, T. Asakura, Interaction of mastoparan with, membranes studied by 1H-NMR spectroscopy in detergent micelles and by solid-state 2H-NMR and 15N-NMR spectroscopy in oriented lipid bilayers, Eur. J. Biochem. 268 (2001) 302–309.
[7] R.L. Gallo, K.M. Huttner, Antimicrobial peptides: an emerging concept in cutaneous biology, J. Investig. Dermatol. 111 (1998) 739–743.
[8] V. Krishnakumari, P. Nagaraj, Antimicrobial and hemolytic activities of Crabolin, a 13-residues peptide from the venom of the European hornet, *Vespa crabro*, and its analogs, J. Pept. Res. 50 (1997) 88–93.
[9] M.A. Mendes, B.M. de Souza, M.R. Marques, M.S. Palma, Structural and biological characterization of two novel peptides from the venom of the neotropical social wasp *Agelaia pallipes pallipes*, Toxicon 44 (2004) 67–74.
[10] H.W. Huang, Action of antimicrobial peptides: two-state model, Biochemistry 39 (2000) 8347–8352.
[11] F.Y. Chen, H.W. Huang, Evidence for membrane thinning effect as the mechanism for peptide-induced pore formation, Biophys. J. 84 (2003) 3751–3758.
[12] K. Matsuzaki, Why and how are peptides–lipid interactions utilized for self defence? Magainins and tachyplesins as archetypes, Biochim. Biophys. Acta 1462 (1999) 1–10.
[13] Z. Oren, Y. Shai, Mode of action of linear amphipathic alpha-helical antimicrobial peptides, Biopolymers 47 (1998) 451–463.
[14] K. Konno, M. Hisada, H. Naoki, Y. Itagaki, N. Kawai, A. Miwa, T. Yasuhara, Y. Morimoto, Y. Nakata, Structure and biological activities of Eumenine Mastoparan-AF (EMP-AF) a new mast cell degranulating peptide in the venom of the solytary wasp (*Anterhynchium flavomarginatum micado*), Toxicon 38 (2000) 1505–1515.
[15] M.L. Sforza, S. Oyama Jr., F. Canduri, C.C.B. Lorenzi, T. Pertinhez, K. Konno, B.M. de Souza, M.S. Palma, J. Ruggiero Neto, W.F. Azevedo Jr., A. Spisni, How C-terminal carboxyamidation alters the biological activity of peptides from the venom of the Eumenine solitary wasp, Biochemistry 43 (2004) 5608–5617.
[16] J.Y. Kim, S.C. Park, M.Y. Yoon, K.S. Hahm, Y. Park, C-terminal amidation of PMAP-23: translocation to the inner membrane of Gram-negative bacteria, Amino Acids 40 (2011) 183–195.
[17] S.R. Dennison, D.A. Phoenix, Influence of C-terminal amidation on efficacy of modelin 5, Biochemistry 50 (2011) 1514–1523.
[18] S.R. Dennison, F. Harris, T. Bhatt, J. Singh, D.A. Phoenix, The effect of C-terminal amidation on the efficacy and selectivity of antimicrobial and anticancer peptides, Mol. Cell. Biochem. 332 (2009) 43–50.
[19] B.M. de Souza, M.S. Palma, Monitoring the positioning of short polycationic peptides in model lipid bilayers by combining hydrogen/deuterium exchange and electrospray mass spectrometry, Biochim. Biophys. Acta 1778 (2008) 2797–2805.
[20] J.A. Demmers, D.T. Rijkers, J. Haverkamp, J.A. Killian, A.J. Heck, Factors affecting gas-phase deuterium scrambling in peptide ions and their implications for protein structure determination, J. Am. Chem. Soc. 124 (2002) 11191–11198.
[21] K. Dohtsu, K. Okumura, K. Hagiwara, M.S. Palma, T. Nakajima, Isolation and sequence analysis of peptides from de venom of *Protonectarina sylveirae* (Hymenoptera—Vespidae), Nat. Toxins 1 (1993) 271–276.
[22] B.M. de Souza, M.A. Mendes, L.D. Santos, M.R. Marques, L.M.M. César, R.N.A. Almeida, F.C. Pagnocca, K. Konno, M.S. Palma, Structural and functional characterization of two novel peptide toxins isolated from the venom of the social wasp *Polybia paulista*, Peptides 26 (2005) 2157–2164.
[23] B.M. de Souza, A.V.R. Silva, V.M.F. Resende, H.A. Arcuri, M.P. dos Santos Cabrera, J. Ruggiero Neto, M.S. Palma, Characterization of two novel polyfunctional mastoparan peptides from the venom of the social wasp *Polybia paulista*, Peptides 30 (2009) 1387–1395.
[24] J. Meletiadis, J.G.M. Meis, J.W. Mouton, J.P. Donnelly, P.E. Verweij, Comparison of NCCLS and 3-(4,5dimethyl-2-thiazyl)-2,5-diphenyl-2H-tetrazolium bromide (MTT) methods of in vitro susceptibility testing of filamentous fungi and development of a new simplified method, J. Clin. Microbiol. 38 (2000) 2949–2954.
[25] G. Rouser, S. Fkeischer, A. Yamamoto, Two dimensional then layer chromatographic separation of polar lipids and determination of phospholipids by phosphorus analysis of spots, Lipids 5 (1970) 494–496.
[26] C.A. Rohl, R.L. Baldwin, Deciphering rules of helix stability in peptides, Methods Enzymol. 295 (1998) 1–26.
[27] Y. Todokoro, I. Yumen, K. Fukushima, S.W. Kang, J.S. Park, T. Kohno, K. Wakamatsu, H. Akutsu, T. Fujiwara, Structure of tightly membrane-bound Mastoparan-X, a G-protein-activating peptide, determined by solid-state NMR, Biophys. J. 91 (2006) 1368–1379.
[28] A.A. Schäffer, L. Aravind, T.L. Madden, S. Shavirin, J.L. Spouge, Y.I. Wolf, E.V. Koonin, S. F. Altschul, Improving the accuracy of PSI-BLAST protein database searches with composition-based statistics and other refinements, Nucleic Acids Res. 29 (2001) 2994–3005.
[29] S.F. Altschul, T.L. Madden, A.A. Schäffer, J. Zhang, Z. Zang, W. Miller, D.J. Lipman, Gapped. BLAST and PSI-BLAST: a new generation of protein database search programs, Nucleic Acids Res. 25 (1997) 3389–3402.
[30] A. Sali, T.L. Blundell, Comparative protein modelling by satisfaction of spatial restraints, J. Mol. Biol. 234 (1993) 779–815.
[31] R.A. Laskowsky, M.W. MacArthur, D.S. Moss, J.M. Thornton, PROCHECK: a program to check the stereochemical quality of protein structures, J. Appl. Crystallogr. 26 (1993) 283–291.
[32] R. Koradi, M. Billeter, K. Wüthrich, MOLMOL: a program for display and analysis of macromolecules structures, J. Mol. Graph. 14 (1996) 51–55.
[33] W. Humphrey, A. Dalke, K. Schulten, VMD: visual molecular dynamics, J. Mol. Graph. 14 (1996) 33–38.
[34] M.A. Mendes, B.M. de Souza, M.S. Palma, Structural and biological characterization of three novel mastoparan peptides from the venom of the neotropical social wasp *Protopolybia exigua* (Saussure), Toxicon 45 (2005) 101–106.
[35] F.W. McLafferty, Z.Q. Guan, U. Haupts, T.D. Wood, N.L. Kelleher, Gaseous conformational structures of Cytochrome C, J. Am. Chem. Soc. 120 (1998) 4732–4740.
[36] D.M. Saidemberg, N.B. Baptista-Saidemberg, M.S. Palma, Chemometric analysis of Hymenoptera toxins and defensins: a model for predicting the biological activity of novel peptides from venoms and hemolymph, Peptides 32 (2001) 1924–1933.
[37] L.D. Santos, J.R.A.S. Pinto, A.R.S. Menegasso, D.M. Saidemberg, A.M.C. Garcia, M.S. Palma, Proteomic profiling of the molecular targets of interactions of the mastoparan Polybia MP-III at the level of endosomal membranes from rat mast cells, Proteomics 12 (2012) 2682–2693.
[38] H. Katayama, T. Ohira, K. Aida, H. Nagasawa, Significance of a carboxyl-terminal amide moiety in the folding and biological activity of crustacean hyperglycemic hormone, Peptides 23 (2002) 1537–1546.
[39] Y. Shai, Mechanism of the binding, insertion and destabilization of phospholipid bilayers membranes by R-helical antimicrobial and cell non-selective lytic peptides, Biochim. Biophys. Acta 1462 (1999) 55–70.
[40] Y. Shai, Mode of action of membrane active antimicrobial peptides, Biopolymers 66 (2002) 236–248.
[41] N. Yokokawa, M. Komatsu, T. Takeda, T. Aizawa, T. Yamada, Mastoparan, a wasp venom, stimulates insulin release by pancreatic islets through pertussis toxin sensitive GTP-binding protein, Biochem. Biophys. Res. Commun. 158 (1989) 712–716.
[42] T. Higashijima, S. Uzu, T. Nakajima, E.M. Ross, Mastoparan, a peptide toxin from wasp venom, mimics receptors by activating GTP-binding regulatory proteins (G proteins), J. Biol. Chem. 263 (1988) 6491–6494.
[43] N.G. Park, Y. Yamato, S. Lee, G. Sugihara, Interaction of mastoparan-B from venom of a hornet in Taiwan with phospholipid bilayers and its antimicrobial activity, Biopolymers 36 (1995) 793–801.
[44] T. Niidome, R. Kawakami, K. Okamoto, N. Ohmori, H. Mihara, H. Aoyagi, Interaction of lipophilic peptides derived from mastoparan with phospholipid vesicles, J. Pept. Res. 50 (1997) 458–464.
[45] B. Orioni, G. Bocchinfuso, J.Y. Kim, A. Palleschi, G. Grande, S. Bobone, Y. Park, J. Kim, K.S. Hahm, L. Stella, Membrane perturbation by the antimicrobial peptide PMAP-23: a fluorescence and molecular dynamics study, Biochim. Biophys. Acta Biomembr. 1788 (2009) 1523–1533.
[46] M. Milik, J. Skolnick, Insertion of peptide chains into lipid membranes: an off-lattice Monte Carlo dynamics model, Proteins Struct. Funct. Genet. 15 (1993) 10–25.